25. CRACK CLOSURE EFFECTS IN STEEL

P. MILLE and G. PLUVINAGE
Laboratoire de Fiabilité Mécanique
Université de METZ, Ile du Saulcy, 57000 METZ, France

The fatigue crack growth mechanism postulates that a crack propagates if it is open only. Since the first reports by ELBER, it is well known that fatigue crack does not always open at minimum load (P_{min}) but a load P_{ouv} generally greater than P_{min}. Only a part of stress intensity factor range is effective (ΔK_{eff}) and many investigators have used this concept to explain the role of environment, overload, R ratio, low ΔK value on fatigue crack growth.

The mechanism of crack opening admits several explanations on the following points :

- crack closure effects result from compressive residual stress produced by reverse plastic zone, ELBER /1/ ;
- the crack opening initiates in the center of the specimen, as experimentally demonstrated by PITONIAK and al /2/, PINEAU /3/, and by finite elements methods achieved by OGURA /4/ and BOZEC /5/;
- before crack opening, the surface contact slowly decreases and this point is clearly shown using potential drop technique. The surface contact starts to decrease at P_r load value ;
- the crack opening is successively followed by crack tip blunting and crack tip shearing which modify the crack tip geometry before load P_{el}.

1 - CRACK CLOSURE MEASUREMENT

Surface displacement, COD and CTOP curves using the clip gauge technique are needed to measure the relative position of these loads (P_r, P_{ouv}, P_{el}). The potential drop technique gives the above particular average of the crack opening situation along the crack front. On this load-displacement diagram (load-surface displacement, load-COD, load-CTOD), a small difference with linear part of curve is shown in the lower part of the diagram. This small difference results in crack closure effects. But the amplitude of the difference depends on position measurement and material properties. It is clearly shown that on COD curves, the crack opening point is easy to detect on stainless steel 316, difficult on construction steel E36 (Fig. 1).

On figure 2 are shown the residual displacement δo and the shaded area representing the closure load intensity. This closure load intensity depends on the surface contact and residual stress. It is possible to increase this closure load by increasing surface contact, for example by environment effect /6/ or by friction in mixed mode of rupture /7/. Generally, these closure loads are too small to be detected with accuracy, load P_{ouv}, and it is necessary to use a differential method /8/. The differential displacement is generally used and defined by $\delta' = \delta - \alpha P$. α is a quantity experimentally adjustable and represents a pseudo-compliance. The experimental determination of P_{ouv} is indicated on figure 2. Using small surface clip gauge and normal clip gauge, we compare crack opening load, P_{ouv}, and surface contact decreasing poing P_r in different situation. The following results are shown in figure 3 :

- The crack opening load in surface ($P_{ouv}^{surface}$) is independant of the measurement point. This point is particularly important for experimental procedure.
- The decreasing surface contact point (P_r) depends on the measurement position.
- The opening point on COD-load diagram (fig. 3a) corresponds to the opening load in the displacement surface-load diagram (figs. 3b to f).

Because of mixture of the decreasing surface contact and different crack front situation, the first linear part on surface displacement curve disappears and it is impossible to determine Pr on this diagram. The crack opening load cannot be determined in the center of the specimen. It is required to use an average value of P_{ouv} and a satisfactory method of determination consists in using the tangent method on differential diagram (see figure 2).

2 - EXPERIMENTAL PROCEDURE

All tests are performed on CT samples, 80 mm wide and 15 mm thick. The conventional clip gauge is used for COD measurement. A special little clip gauge 2 mm wide is used for surface and inside CTOD measurements. Three types of steel are tested :

- Stainless steel 316 - yield strength σ_y = 225 MPa
- High strength steel 35NCD 16 σ_y = 1600 MPa
- Construction steel E36 σ_y = 410 MPa

3 - INFLUENCE OF CRACK LENGTH ON CRACK CLOSURE

A test was performed on 35NCD16 steel with the following conditions :

ΔK = (constant about 2 %) 22MPa$\sqrt{m}$ at R = 0,1

It is shown that the effective stress intensity factor range ΔK_{eff} does not vary during the test, figure 4 :

$$0.3 < o/w < 0.6$$

It does not seem that the abrasing or compressive effects affect the crack closure effect as suggested elsewhere /9/ for long cracks.

4 - INFLUENCE OF LOAD RATIO R AND MAXIMUM STRESS INTENSITY FACTOR KMAX ON EFFECTIVE STRESS INTENSITY FACTOR MODULUS U

The variations of modulus U with Kmax at different R values are represented in figure 5 for 35NCD16 high strength steel. We see that modulus U increases slowly to reach U = 1, when Kmax increases and decreases quickly at the beginning of crack propagation stade I (K_{max} Low 12MPa$\sqrt{m}$). Similar curves were obtained by KIKUKAWA and al. /10/. For R value greater than 0.4, U reaches rapidly the unit value. When the crack closure load is below the minimum load, any closure effect can be detected. This situation is produced for 0.3 < R < 0.4 and is called "R cut value". In stade II of crack propagation, the curves seem parallel. For this reason a linear relation can be approximately found between U and R values like ELBER's relation U = 0.4 + 0.5 R. For this type of steel, the crack growth rate is about 10^{-6}mm/cycle with ΔK equal to 10MPa$\sqrt{m}$. It seems that the extrapolation $U \rightarrow 0$ gives a constant Kmax value for all curves with different R ratio. U = 0 has a physical meaning : at threshold, the crack is not open and does not propagate. In the author's opinion, this method is a good estimation for fatigue threshold ΔK_s and is rapidly obtained when the crack growth rate reaches 10^{-6} mm/cycle. For example, we measured the fatigue threshold with conventional procedure (step by step decreasing load method) in stainless steel 316 and we found 6MPa$\sqrt{m}$ = ΔK_s for $da/dN = 10^{-7}$mm/cycle. In figure 6 we stopped experimental procedure at 2.3 10^{-6}mm/cycle, ΔK = 10.1 MPa$\sqrt{m}$ and by extrapolation with U = 0, we obtained the same value : 6 MPa$\sqrt{m}$. This method requires some more investigations for a large validity. We remarked that for a threshold value, Kmax seemed to be constant with different R values. This point agrees with SCHMIDT and PARIS assumptions /11/ to explain the linear relation between fatigue threshold and R value $\Delta K_s = \Delta K_{so}(1-R)$. Unfortunately, for the lowest value of crack growth rate, the crack seems always open in steels. It appeared that we found the same situation in aluminium alloys for crack growth rate equal to 10^{-7}mm/cycle /12/.

5 - ENVIRONMENT EFFECT ON CRACK CLOSURE

In salt water, the crack growth rate is accelerated by a factor three to five as it can be seen in construction steel, i.e. E36 steel. Several mechanisms have been proposed to explain this acceleration of the crack growth rate : dissolution of metal at crack tip, hydrogen embrittlement, modification of cyclic plasticity at crack tip, wedge effect due to corrosion products. These types of steels are not sensitive to hydrogen embrittlement (low carbon steels). The alteration of cyclic plasticity at crack tip or wedge effect modify the residual stress and crack closure effect consequently. Experimentally it is impossible to notice a modification on crack closure load. The important modification that appears is increasing the closure energy (represented by the dashed area between the linear part and the real curves). This "closure energy" do not increase by modification of closure load but by residual displacement δo, figure 7. This increasing of residual displacement is due to corrosion products. The "closure energy" increases in function of time and reaches a plateau. Then, the chemical corrosion reaction is rapid enough to occur with all chemical contents produced by "crack pumping effects".

6 - CHANGE IN CRACK CLOSURE FOLLOWING AN OVERLOAD

Following an overload, the crack is delayed or stopped. The number of retardation cyles is a complex function of the overload ratio, type of overload (single or block), yield strength etc ... For a single tension overload, there is generally a good correlation between the overload plastic zone and the affected crack length. Several modifications can follow an overload : in crack tip geometry, strain hardening materials and crack closure effect. It seems that the crack tip geometry recovers its initial shape in a very few cycles.
In figure 8, it is shown that in 20-30 cycles, the hysteresis loop width decreases quickly to recover its initial shape. The strain hardening effect tends to lower the crack closure one, as demonstrated by SCHISVE /13/ in aluminium alloys. Several models, e.g. TREBULE's models /14/ explain overload retardation by the increasing of crack closure load and consequently, the decreasing of stress intensity factor rang
In figure 9, we have followed the crack growth rate on E36 steel after an overload and simultaneously crack closure load during crack passing through the overload plastic zone. These curves are similar to that residual stress curves found by KLESNIL and LUCAS /15/. These authors have calculated these residual stress by F.E.M. and have got experimental results using the XRay microbeam method. However it seems difficult to recover the initial crack closure value, this may be explained by the fact that crack closure appears to be sensitive to memory effect.

7 - CONCLUSION

The surface opening load $P_{ouv}^{surface}$ can be measured on CTOD load curves and COD load curve.

The decreasing surface contact load can only be measured on CTOD load curves and depends on the position measurement.

The Kmax value affects the closure load and $U \rightarrow 0$ appears to be a good estimation of the fatigue threshold value ΔK_s

The crack closure effect does not explain the environment effect but the "closure energy" seems in relation with the surface contact.

The overload retardation seems to be partially explained by the crack closure effect. But crack closure is affected after overload by the memory effect.

REFERENCES

1 ELBER W.
The significance of fatigue crack closure
ASTM STP 486 1971 p. 230

2 PITONIAK I.J.
Eng. Fracture Mechanics 7 (1975) 705-711

3 Seuil de non-fissuration en fatigue
Contrat DGRST N° 75.711.50

4 OGURA K - OHJI K.
F.E.M. analysis of crack closure and delay in fatigue crack growth under variable amplitude loading - Eng. Fracture Mechanics - vol. 9, 1977, p. 471-480

5 BOZEC J.
Propagation d'une fissure de fatigue dans une éprouvette de flexion
Thèse BORDEAUX, 1977

6 NOUAIL G. - PLUVINAGE G.
Etude de l'influence des inhibiteurs de corrosion sur la vitesse de fissuration d'un acier de construction en eau salée
Ecole d'Eté sur la fatigue, SHERBROOKE, 1978

7 HOURLIER F.- PINEAU A.
Recherche d'un critère donnant la direction de propagation des fissures de fatigue sous chargement polymodal
Ecole d'Eté sur la fatigue, SHERBROOKE, 1978

8 ROBIN C - DOMINIAK S. - PLUVINAGE G.
Variation of crack opening load diagram with fatigue crack growth rate
Mat. Sci. Eng. vol. 29, 1977, pp. 145-150

9 VON EW-HERTZBERG Roberts
ASTM SPT 513 - 230, 1972

10 KIKUKAWA M. - MASAHIRO JONO - TANAKA K.
Fatigue crack closure behavior at low stress intensity level
Proc. of the 2nd Int. Conf. on Mech. Behavior of Materials, BOSTON, 1976

11 SCHMIDT R.A. - PARIS P.C.
Threshold for fatigue crack propagation and the effect of load ratio and frequency - ASTM STP 536, 1973, p. 79

12 ROBIN C.
Comportement au seuil de non-fissuration en fatigue de l'alliage d'aluminium AU2GN - Thèse METZ, 1978

13 SCHISVE J.
Observation on the prediction of fatigue crack growth propagation under variable amplitude moad.
STP 595, p. 326

14 TREBULES V.W.- ROBERTS and HERTZBERG G.R.W.
Effect of multiple overloads on fatigue crack propagation in 2024 TB aluminium alloy ASTP STP 536, 1973, p. 115

15 KUNZ L. - KLESNIL Z. - LUKAS P.
Kovové materials 5 15 Bratislava, 1977, pp. 556-570

FIGURE CAPTION

Figure 1 Load displacement diagram showing the residual displacement δo and closure load intensity

Figure 2 Differential diagram used to determine with more accuracy, the opening load P_{ouv}

Figure 3 Influence of the position measurement on the opening load P_{ouv}

Figure 4 Influence of the crack length on the opening load P_{ouv}

Figure 5 Variation of $U = \Delta K_{eff}/\Delta K$ versus K_{max} for different R values

Figure 6 Extrapolation method to find the threshold value in 316 stainless steel

Figure 7 Increasing of the closure energy by corrosion products in construction steel.

Figure 8 Evolution of the hysteresis loop during the overload retardation.

Figure 9 Evaluation of the closure load and fatigue crack growth during the overload retardation.

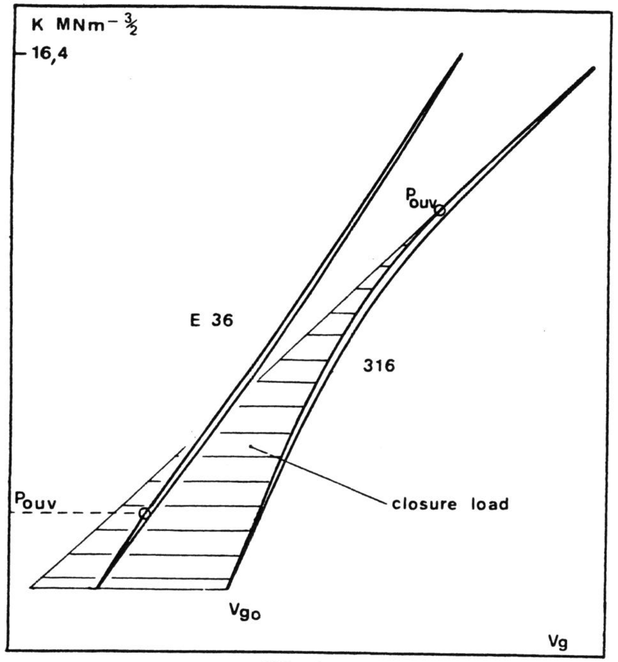
K MNm$^{-3/2}$
16,4
P_{ouv}
E 36
316
P_{ouv}
closure load
V_{go}
Vg

FIG. 1

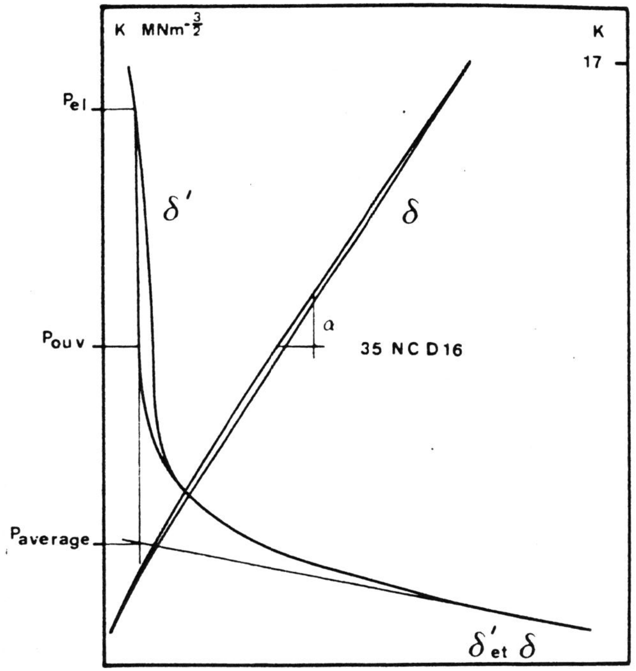
K MNm$^{-3/2}$
K
17
P_{el}
δ'
δ
α
P_{ouv}
35 NC D16
$P_{average}$
δ' et δ

FIG. 2

FIG. 3

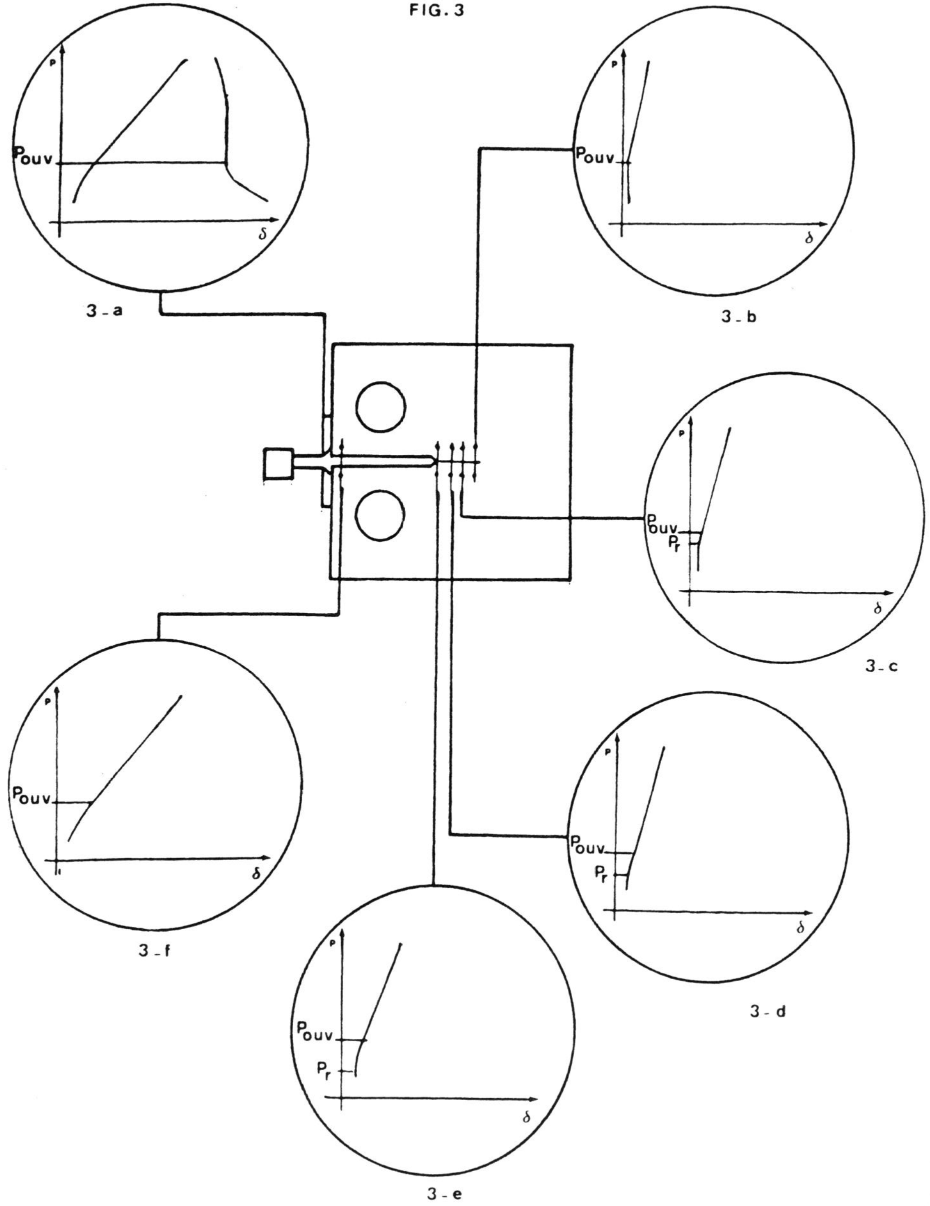

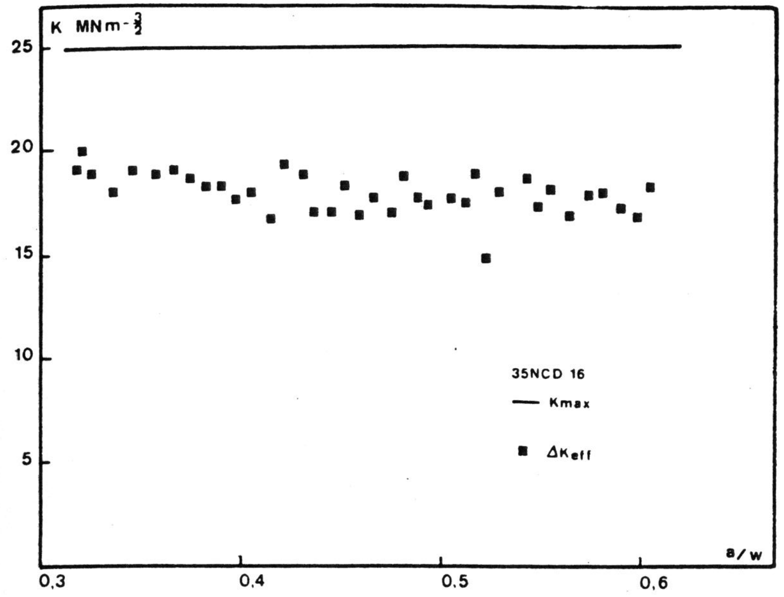

FIG. 4

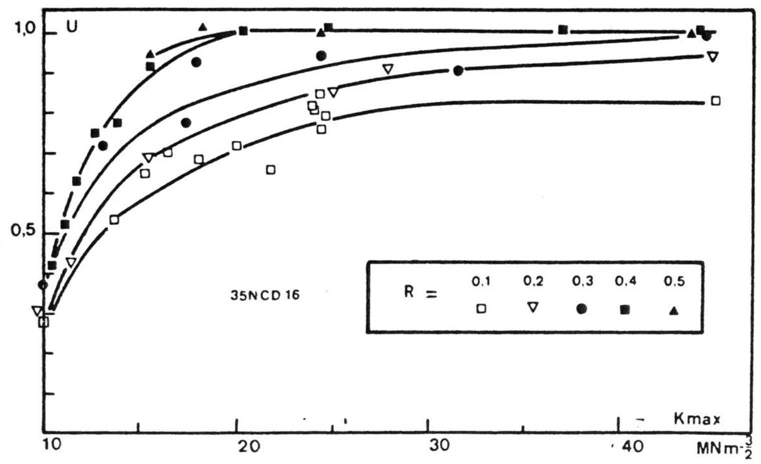

FIG. 5

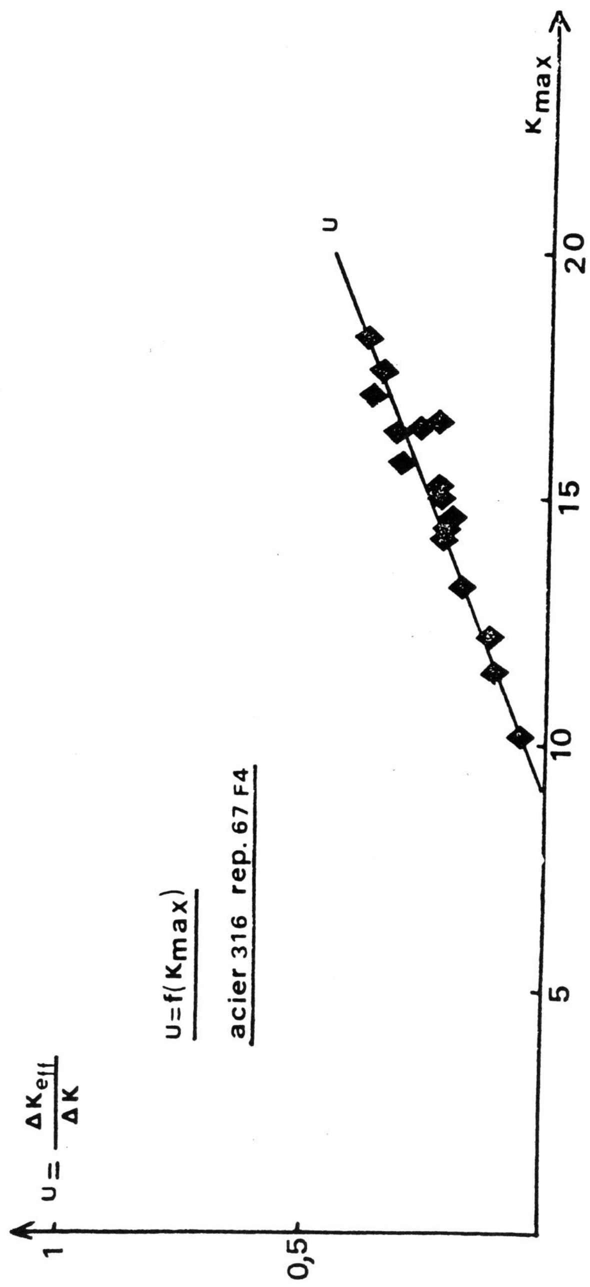
U = ΔKeff / ΔK
U=f(Kmax)
acier 316 rep. 67 F4
U
Kmax
1
0,5
5
10
15
20

FIG. 6

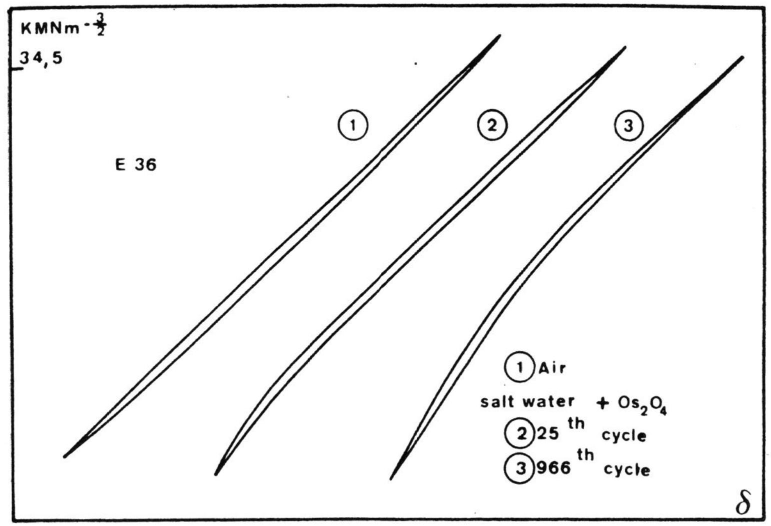
KMNm-3/2
34,5
E 36
1
2
3
1 Air
salt water + Os2O4
2 25 th cycle
3 966 th cycle
δ

FIG. 7

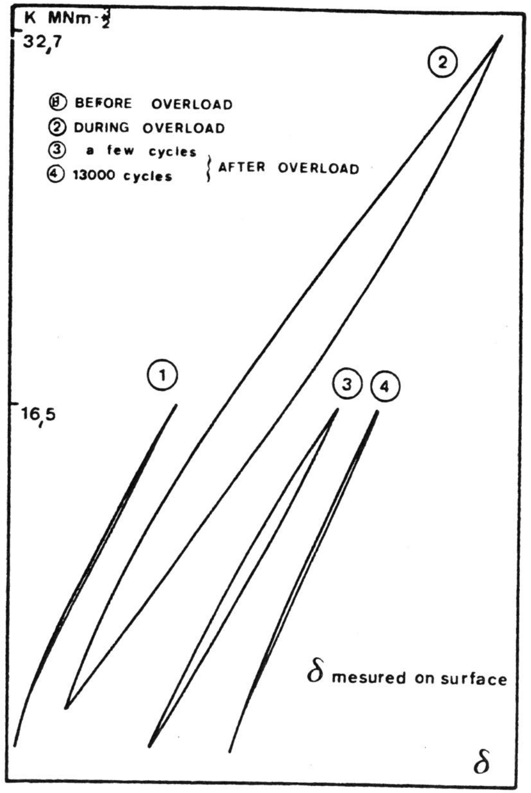
K MNm
32,7
16,5
BEFORE OVERLOAD
DURING OVERLOAD
a few cycles
13000 cycles
AFTER OVERLOAD
1
2
3
4
δ mesured on surface
δ

FIG. 8

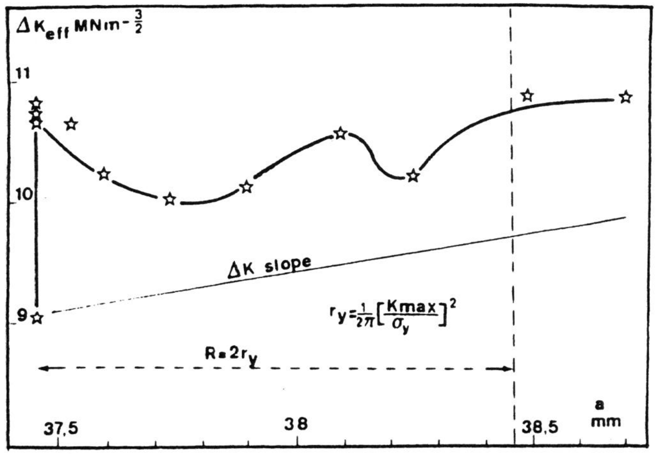
ΔK eff MNm
11
10
9
ΔK slope
R=2r
37,5
38
38,5
a
mm

9-a

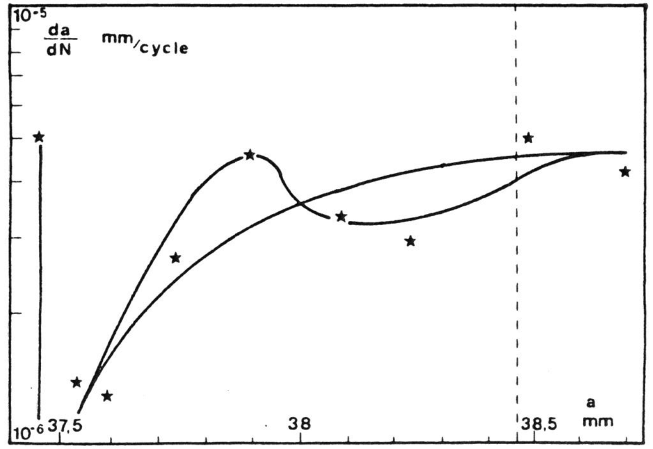
10
da
dN
mm/cycle
37,5
38
38,5
a
mm

9-b